available at www.sciencedirect.com
journal homepage: www.europeanurology.com

European Association of Urology

Platinum Priority – Brief Correspondence – Prostate Cancer

Editorial by Shawn E. Lupold, William B. Isaacs, Jun Luo on pp. 461–462 of this issue

Grade Group 1 Prostate Cancers Exhibit Tumor-defining Androgen Receptor–driven Programs

Simon Linder[a], *Tesa M. Severson*[a,b], *Koen J.C. van der Mijn*[c], *Ekaterina Nevedomskaya*[a,b], *Joseph C. Siefert*[a,b], *Suzan Stelloo*[a], *Mark M. Pomerantz*[d], *Matthew L. Freedman*[e,f], *Henk van der Poel*[f,g], *Carmen Jerónimo*[h,i,j], *Rui Henrique*[h,i,j], *Andries M. Bergman*[c,k,*], *Wilbert Zwart*[a,l,*]

[a] *Division of Oncogenomics, Oncode Institute, The Netherlands Cancer Institute, Amsterdam, The Netherlands;* [b] *Division of Molecular Carcinogenesis, Oncode Institute, The Netherlands Cancer Institute, Amsterdam, The Netherlands;* [c] *Division of Medical Oncology, The Netherlands Cancer Institute, Amsterdam, The Netherlands;* [d] *Department of Medical Oncology, Dana-Farber Cancer Institute, Harvard Medical School, Boston, MA, USA;* [e] *The Eli and Edythe L. Broad Institute, Cambridge, MA, USA;* [f] *Division of Urology, The Netherlands Cancer Institute, Amsterdam, The Netherlands;* [g] *Department of Urology, Amsterdam University Medical Centers, Amsterdam, The Netherlands;* [h] *Cancer Biology and Epigenetics Group, Research Center of the Portuguese Oncology Institute of Porto, Porto, Portugal;* [i] *Department of Pathology, Portuguese Oncology Institute of Porto, Porto, Portugal;* [j] *Department of Pathology and Molecular Immunology, School of Medicine and Biomedical Sciences, University of Porto, Porto, Portugal;* [k] *Division of Oncogenomics, The Netherlands Cancer Institute, Amsterdam, The Netherlands;* [l] *Laboratory of Chemical Biology and Institute for Complex Molecular Systems, Department of Biomedical Engineering, Eindhoven University of Technology, Eindhoven, The Netherlands*

Article info

Article history:
Accepted May 23, 2023

Associate Editor:
Todd M. Morgan

Keywords:
Androgen receptor
Epigenomics
Gleason grading
International Society of Urological Pathology grade groups
Prostate cancer
Transcriptomics

Abstract

Grade group 1 (GG1) primary prostate cancers with a pathologic Gleason score of 6 are considered indolent and generally not associated with fatal outcomes, so treatment is not indicated for most cases. These low-grade cancers have an overall negligible risk of locoregional progression and metastasis to distant organs, which is why there is an ongoing debate about whether these lesions should be reclassified as "noncancerous". However, the underlying molecular activity of key disease drivers, such as the androgen receptor (AR), have thus far not been thoroughly characterized in low-grade tumors. Therefore, we set out to delineate the AR chromatin-binding landscape in low-grade GG1 prostate cancers to gain insights into whether these AR-driven programs are actually tumor-specific or are normal prostate epithelium-like. These analyses showed that GG1 tumors do not harbor a distinct AR cistrome and, similar to higher-grade cancers, AR preferentially binds to tumor-defining cis-regulatory elements. Furthermore, the enhancer activity of these regions and the expression of their respective target genes were not significantly different in GG1 tumors. From an epigenetic perspective, this finding supports the cancer designation currently given to these low-grade tumors and clearly distinguishes them from noncancerous benign tissue.

Patient summary: We characterized the molecular activity of the androgen receptor protein, which drives prostate cancer disease, in low-grade tumors. Our results show that

* Corresponding authors. The Netherlands Cancer Institute, Plesmanlaan 121, 1066 CX Amsterdam, The Netherland. Tel. +31 20 512 2920 (A.M. Bergman); Tel. +31 20 5122101 (W. Zwart).
E-mail addresses: a.bergman@nki.nl (A.M. Bergman), w.zwart@nki.nl (W. Zwart).

https://doi.org/10.1016/j.eururo.2023.05.032

these tumors are true cancers and are clearly separate from benign prostate tissue despite their low clinical aggressiveness.

Adenocarcinoma of the prostate (PCa) is the second most common cancer among men, with almost 1.5 million new diagnoses annually [1]. Most patients present with organ-confined disease, which can potentially be cured with locoregional therapies such as surgery (radical prostatectomy) or radiotherapy. However, approximately 30% of these patients will experience a rise in serum prostate-specific antigen (PSA), which is referred to as biochemical recurrence (BCR) and indicates tumor relapse. At the time of PCa diagnosis, tumor biopsies are histologically graded using the Gleason system [2], which helps in predicting patient prognosis. The Gleason score (GS) describes the two most common cell morphologies according to their differentiation status and ranges from GS 6 (lowest grade; International Society for Urological Pathology [ISUP] grade group 1 [GG1]) to GS 9–10 (highest grades; ISUP GG5). However, there is ongoing debate regarding whether low-grade GG1 lesions should be considered cancerous or as benign neoplasms given their overall low risk of metastasis [3]. It remains unclear how best to classify GG1 lesions from a biological perspective: do they resemble noncancerous prostate tissue or do they share characteristics of higher-grade PCa? We set out to characterize the chromatin-binding landscape of the androgen receptor, the main driver of PCa development and progression [4], in GG1 tumors to gain a better understanding of whether AR-driven programs in these low-grade lesions are more similar to normal tissue or exhibit tumor specificity.

To address this, we analyzed AR chromatin immunoprecipitation sequencing (ChIP-seq) data obtained for primary PCa specimens from radical prostatectomy in 82 patients [5]. These covered the entire spectrum of ISUP grade groups (GG1, n = 17; GG2, n = 31; GG3, n = 11; GG4, n = 7; GG5, n = 16) and showed a trend towards the expected increase in BCR rate with increasing GS (Fig. 1A, Supplementary material), from the highest rate in GG5 to the lowest in GG1 (odds ratio 4.58, p = 0.076, Fisher's exact test; risk difference 37.5%, 95% confidence interval 5.4–69.6%). The expected molecular features were observed, such as fusions of the *ERG* oncogene in half (51%) of the cohort (Supplementary Fig. 1A, B) and lower expression of the tumor suppressor *PTEN* in patients with higher-grade disease (Supplementary Fig. 1C–E). We then integrated the AR cistromics (Fig. 1A) with ChIP-seq data on the active enhancer and promoter histone mark H3K27ac (Supplementary Table 1) as well as gene expression data (RNA-seq) obtained from the same clinical specimens (Supplementary Table 2). To assess whether GG1 tumors harbor a distinct AR cistrome, we performed an unsupervised differential binding analysis on all AR ChIP-seq samples. This revealed no obvious clustering by grade group (Fig. 1B, C) and largely overlapping chromatin-binding intervals (Fig. 1D and Supplementary Fig. 2A, B) and motif enrichment (Fig. 1E), suggesting that, on the basis of AR-chromatin interactions, GG1 tumors do not seem to represent a different biological entity to higher-grade lesions. Supervised analyses directly comparing GG1 and GG5 lesions revealed a subset of GG1-enriched binding sites (Supplementary Fig. 2C and Supplementary Table 3) that showed no meaningful overlap with AR sites specific to normal prostate epithelium (Supplementary Fig. 2D). These data indicate that GG1-specific AR-regulated enhancers are distinctly different from cis-regulatory elements found in healthy tissue.

Given the importance of AR in driving context-dependent epigenomic and transcriptional programs that characterize normal prostate epithelium, primary tumors, and metastatic lesions, we next investigated whether genome-wide AR binding in GG1 specimens is enriched for AR binding-site (ARBS) profiles that hallmark a tumor (T) versus normal (N) state (Supplementary Table 4 [6]). While healthy prostate tissue was strongly enriched for the N-ARBS signal, GG1 lesions showed strongest AR binding at T-ARBS (Fig. 1F, G), representing phenotype copies of the profiles observed in high-grade GG5 samples

Fig. 1 – AR chromatin binding landscape in GG1 tumors is enriched in tumor-defining regulatory elements. (A) Study design and cohort overview. Multi-omics profiling of (1) androgen receptor (AR) chromatin immunoprecipitation sequencing (ChIP-seq), (2) H3K27ac ChIP-seq, and (3) gene expression profiling (RNA-seq) was performed on prostate cancer tissue specimens from 82 patients [5]. The plot shows the proportion of patients with biochemical recurrence (BCR) stratified by International Society of Urological Pathology (ISUP) grade group. (B) Correlation heatmap for peak AR occupancy. Clustering of the samples (n = 82) is based on all called peaks and represents Pearson correlations between individual ChIP-seq samples. Colored column bars indicate the grade group (GG1, GG2, GG3, GG4, GG5) and BCR status (controls, cases, not available [NA]). (C) Principal component analysis plot for peak AR occupancy. Each dot represents a ChIP-seq sample, colored to represent the grade group. (D) Venn diagram indicating the overlap of AR binding sites between GG1 and GG5 ChIP-seq samples, highlighting grade group–specific and common binding sites. For each group, the union of identified peaks was included. (E) Dot plot representing motif enrichment (z-score) at GG1-specific, GG1/GG5-common and GG5-specific AR binding sites (Fig. 1D). Dots are colored according to the motif and are sized according to significance (p value). (F) Profile plots (top) and tornado plots (bottom) showing the AR ChIP-seq signal at normal (N; n = 2690), tumor (T; n = 9181) and metastasis (Met; n = 17 626) AR binding sites (ARBS) in GG1 tumors by BCR status (left, controls: no BCR within 10 yr after diagnosis; right, cases: BCR within 5 yr after diagnosis) in comparison to a healthy prostate epithelium sample and a GG5 tumor (P268T) as controls. Data are centered at ARBS depicting a 1-kb window around the peak center. The y-axes for profile plots and color scale indicate the ChIP-seq signal in reads per genomic content (RPGC). (G) Boxplot indicating AR ChIP-seq counts in GG1 tumors at N-ARBS, T-ARBS and Met-ARBS. ****p < 0.0001 (two-sample t test). (H) Scatterplot showing Pearson correlation (R = 0.89, p < 0.0001) of AR ChIP-seq counts at T-ARBS between low-grade GG1 and high-grade GG5 tumors. The linear trend with 95% confidence interval is shown. (I) Profile plots indicating the AR ChIP-seq signal (RPGC) in GG1 tumors from cases and controls at N-ARBS (left), T-ARBS (middle) and Met-ARBS (right).

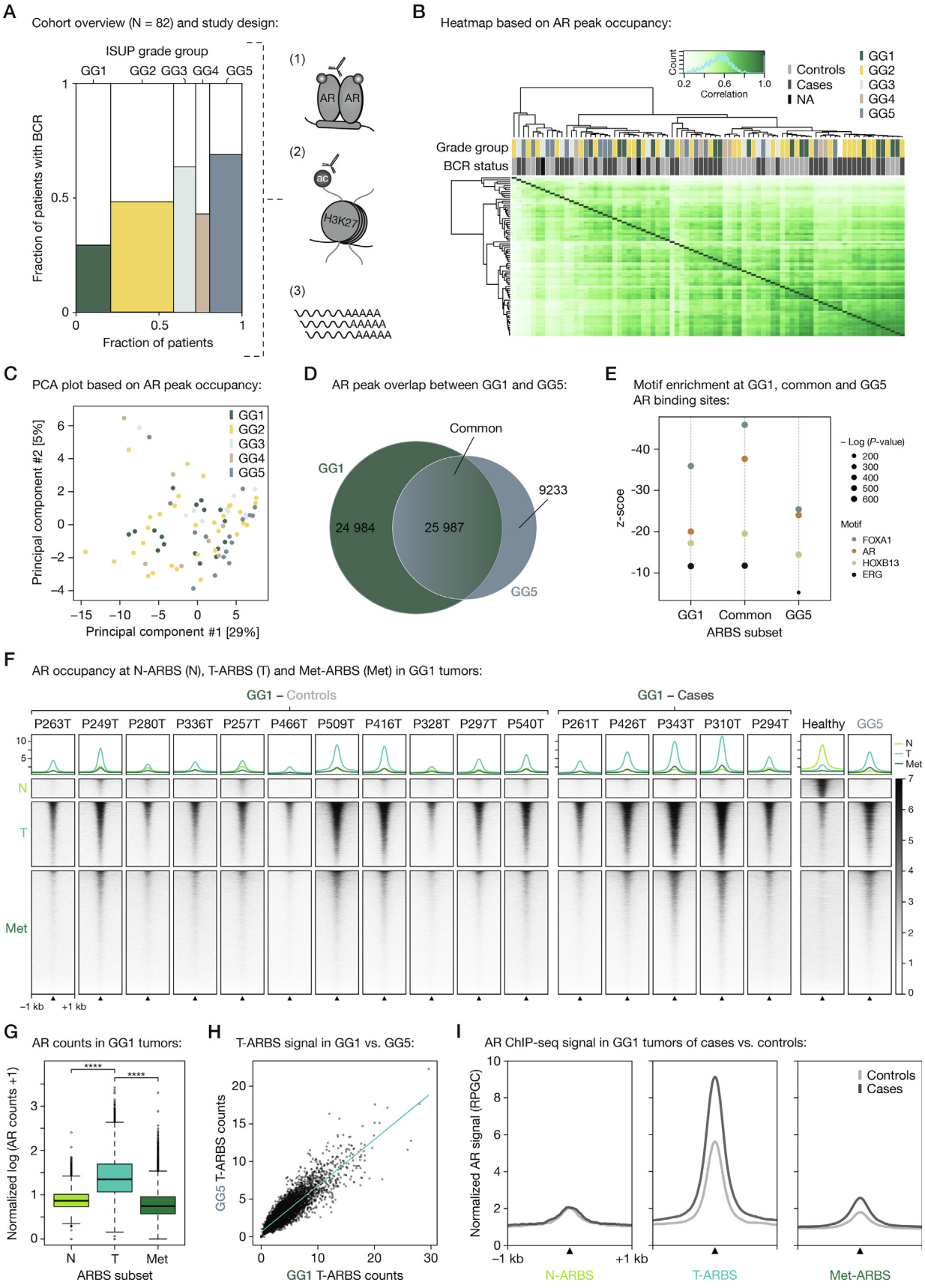

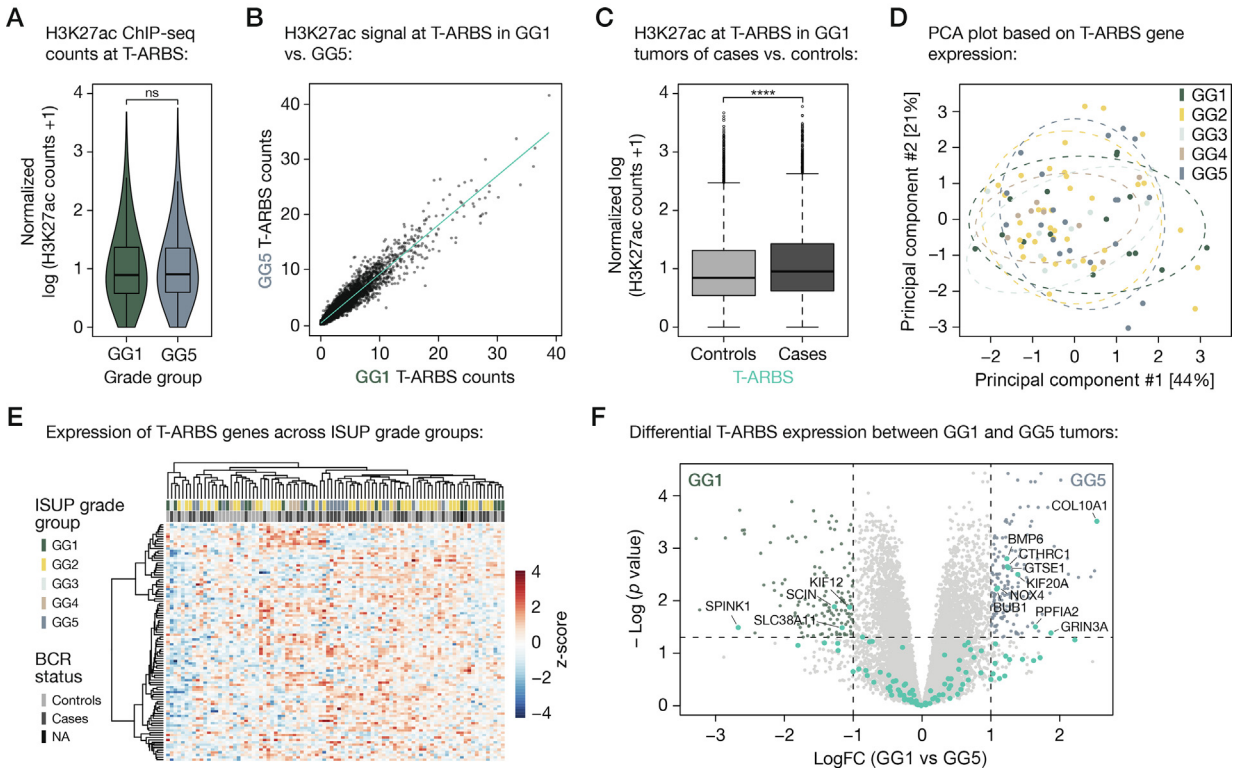

Fig. 2 – Enhancer activity and gene expression of tumor-specific androgen receptor (AR) targets are highly comparable between low-grade and high-grade prostate cancers. (A) Violin plot indicating the H3K27ac chromatin immunoprecipitation sequencing (ChIP-seq) signal at tumor AR-binding sites (T-ARBS) of grade group 1 (GG1) and GG5 tumors. ns, $p > 0.05$ (two-sample *t* test). (B) Scatterplot showing Pearson correlation ($R = 0.96$, $p < 0.0001$) of H3K27ac ChIP-seq counts at T-ARBS between low-grade GG1 and high-grade GG5 tumors. The linear trend with 95% confidence interval is shown. (C) Boxplot indicating H3K27ac ChIP-seq counts at T-ARBS in GG1 tumors from cases (biochemical recurrence [BCR] within 5 yr after diagnosis) and controls (no BCR within 10 yr after diagnosis). ****$p < 0.0001$ (paired *t* test). (D) Principal component analysis plot for expression of a T-ARBS gene set [8]. Each dot represents an RNA-seq sample ($n = 91$) colored according to grade group. Ellipses denote the 80% confidence interval. (E) Unsupervised hierarchical clustering of RNA-seq samples according to the expression of T-ARBS genes. The color scale indicates gene expression (z-score) and the colored column bars indicate the grade group (GG1, GG2, GG3, GG4, GG5) and BCR status (controls, cases, not available [NA]) per sample. (F) Volcano plot depicting differential gene expression between low-grade GG1 (left) and high-grade GG5 tumors (right). Significantly differentially expressed genes and T-ARBS genes are highlighted. Significance cutoffs are shown as dotted lines (log fold-change [FC] between GG1 and GG5 ≥1; $p \leq 0.05$), and T-ARBS genes exceeding this threshold are labeled.

(Fig. 1H). These data further demonstrate that low-grade GG1 lesions harbor genomic AR programs that define tumor rather than healthy prostate epithelium. Since our cohort included patients with GG1 tumors that either did or did not develop BCR within 5 yr after diagnosis (cases and controls, respectively; Fig. 1A), we hypothesized that cases that later relapsed might be enriched for tumor-specific T-ARBS and particularly for a more late-stage metastasis-specific ARBS (Met-ARBS) signal [7]. To test this hypothesis, we also assessed the AR chromatin occupancy at Met-ARBS (Fig. 1F). Although the overall signal was rather low, as expected for primary disease (Fig. 1G), we did observe a significantly higher signal at these more aggressive metastatic binding sites in GG1 cases versus GG1 controls, accompanied by a higher T-ARBS signal and no difference in N-ARBS signal (Fig. 1I). Notably, while the enrichment for T-ARBS and Met-ARBS signals was detected in both GG1 cases and GG1-controls, the signal strength at these tumor-specific ARBS was significantly elevated in patients with future relapse and could help in identifying and stratifying these cases (Fig. 1F, G, I, Supplementary Fig. 3A–C, and Supplementary Fig. 4A).

Taken together, our analyses reveal that low-grade GG1 lesions do not harbor a distinct healthy prostate epithelium–like AR chromatin-binding landscape that could explain their favorable prognosis, but are rather enriched for tumor-defining AR-driven programs, similar to the situation for higher-grade tumors.

We next investigated whether AR binding to T-ARBS was accompanied by changes in the activity of these cis-regulatory elements and the target genes under their control. To this end, we examined the H3K27ac signal at T-ARBS, which revealed highly comparable signal strength between low-grade GG1 and high-grade GG5 lesions (Fig. 2A, B). Similar to the higher AR signals in GG1 cases versus GG1 controls, we observed elevated H3K27ac at T-ARBS (Fig. 2C) in cases versus controls, while H3K27ac at N-ARBS and Met-ARBS was lower and higher, respectively (Supplementary Fig. 4B).

Having shown the prevalence of tumor-defining genomic features in low-grade lesions, we sought to characterize whether expression of the distal associated target genes could stratify GG1 tumors from higher-grade lesions. We used a T-ARBS gene set we previously identified that was

generated by integrating differential gene expression with AR chromatin profiles gained during tumorigenesis [8]. However, the expression of these tumor-specific AR-driven genes (n = 102; Supplementary Table 5) did not separate GG1 samples from higher-grade lesions (Fig. 2D), but rather clustered them independent of their grade group (Fig. 2E) and revealed lower expression in GG1 controls and higher expression in GG1 cases (Supplementary Fig. 5A–C). Similarly, analysis of differential gene expression between GG5 and GG1 tumors (Supplementary Table 6) revealed enrichment of expected gene sets for high-grade (eg, epithelial-mesenchymal transition and cell cycle–related gene ontology terms) or low-grade lesions (eg, metabolic pathways and canonical—not tumor-specific—androgen response), clearly highlighting the aggressiveness of poorly differentiated high-risk disease (Supplementary Fig. 5D–F). However, overlay of the expression of tumor-determining AR-regulated genes revealed no significant difference in the expression of most of the T-ARBS genes (89/102) between these grade groups (Fig. 2F), further illustrating that low-grade lesions express tumor-specific gene sets. Overall, these analyses demonstrate that both the tumor-specific cistromic activity and the transcriptomic activity of AR in low-grade lesions is not enriched for signaling specific to normal prostate epithelium, and instead shows high concordance with high-grade prostate cancer.

Although higher-grade tumors exhibit molecular characteristics not observed in low-grade lesions, ultimately resulting in their more aggressive phenotype and poorer clinical outcomes, GG1 tumors are clearly distinguishable from healthy prostate epithelium. Previous studies have shown that GG1 tumors share morphological features with higher-grade Gleason patterns, and genomic alterations such as *PTEN* deletions and *MYC* amplifications that are typically enriched in aggressive PCa can be detected in these low-grade samples [9,10]. We now provide evidence that the epigenetic features of the prostate cancer driver AR that hallmark primary adenocarcinomas as opposed to normal prostate epithelium, along with the genes it controls, are not distinct in GG1 tumors but are actually highly comparable between low-grade and high-grade disease, positioning GG1 (Gleason 6) lesions as bona fide cancers from an epigenetic perspective.

Author contributions: Wilbert Zwart had full access to all the data in the study and takes responsibility for the integrity of the data and the accuracy of the data analysis.

Study concept and design: Linder, Zwart, Bergman.
Acquisition of data: Stelloo.
Analysis and interpretation of data: Linder, Nevedomskaya, Severson, Siefert.
Drafting of the manuscript: Linder, Zwart, Bergman.
Critical revision of the manuscript for important intellectual content: van der Poel, van der Mijn.
Statistical analysis: Linder, Nevedomskaya, Severson.
Obtaining funding: Zwart, Bergman, Henrique, Jerónimo, Pomerantz, Freedman.
Administrative, technical, or material support: Siefert, Stelloo, Henrique, Jerónimo.
Supervision: Zwart, Bergman, Henrique, Jerónimo.
Other: None.

Financial disclosures: Wilbert Zwart certifies that all conflicts of interest, including specific financial interests and relationships and affiliations relevant to the subject matter or materials discussed in the manuscript (eg, employment/affiliation, grants or funding, consultancies, honoraria, stock ownership or options, expert testimony, royalties, or patents filed, received, or pending), are the following: None.

Funding/Support and role of the sponsor: This work was supported by Movember (NKI01 to A.M. Bergman and W. Zwart), the KWF Dutch Cancer Society (10084 ALPE to A.M. Bergman and W. Zwart), a KWF Dutch Cancer Society/Alpe d'HuZes Bas Mulder Award (NKI 2014-6711 to W. Zwart), The Netherlands Organization for Scientific Research (NWO-VIDI-016.156.401 to W. Zwart), and the US Department of Defense (W81XWH-19-1-0565 to M.M. Pomerantz, M.L. Freedman and W. Zwart). The sponsors played a role in the design and conduct of the study and data collection.

Acknowledgments: We would like to thank the NKI Genomics Core Facility for bioinformatics support, and the NKI Research High Performance Computing facility for computational infrastructure. We also thank all the members of the Zwart/Bergman laboratory for fruitful discussions and technical advice. Finally, we would like to thank Peter S. Nelson (Divisions of Human Biology and Clinical Research, Fred Hutchinson Cancer Research Center, Seattle, WA, USA) for bringing this open debate to our attention and for his valuable input to the manuscript.

Peer Review Summary

Peer Review Summary and Supplementary data to this article can be found online at https://doi.org/10.1016/j.eururo.2023.05.032.

References

[1] Sung H, Ferlay J, Siegel RL, et al. Global cancer statistics 2020: GLOBOCAN estimates of incidence and mortality worldwide for 36 cancers in 185 countries. CA Cancer J Clin 2021;71:209–49.
[2] Gleason DF, Mellinger GT. Prediction of prognosis for prostatic adenocarcinoma by combined histological grading and clinical staging. J Urol 1974;111:58–64.
[3] Ross HM, Kryvenko ON, Cowan JE, Simko JP, Wheeler TM, Epstein JI. Do adenocarcinomas of the prostate with Gleason score (GS) ≤6 have the potential to metastasize to lymph nodes? Am J Surg Pathol 2012;36:1346–52.
[4] Stelloo S, Bergman AM, Zwart W. Androgen receptor enhancer usage and the chromatin regulatory landscape in human prostate cancers. Endocr Relat Cancer 2019;26:R267–85.
[5] Stelloo S, Nevedomskaya E, Kim Y, et al. Integrative epigenetic taxonomy of primary prostate cancer. Nat Commun 2018;9:4900.
[6] Pomerantz MM, Li F, Takeda DY, et al. The androgen receptor cistrome is extensively reprogrammed in human prostate tumorigenesis. Nat Genet 2015;47:1346–51.
[7] Pomerantz MM, Qiu X, Zhu Y, et al. Prostate cancer reactivates developmental epigenomic programs during metastatic progression. Nat Genet 2020;52:790–9.
[8] Severson T, Qiu X, Alshalalfa M, et al. Androgen receptor reprogramming demarcates prognostic, context-dependent gene

sets in primary and metastatic prostate cancer. Clin Epigenet 2022;14:60.
[9] Carter HB, Partin AW, Walsh PC, et al. Gleason score 6 adenocarcinoma: should it be labeled as cancer? J Clin Oncol 2012;30:4294–6.
[10] Gandellini P, Casiraghi N, Rancati T, et al. Core biopsies from prostate cancer patients in active surveillance protocols harbor PTEN and MYC alterations. Eur Urol Oncol 2019;2:277–85.